International Journal of Biometeorology
https://doi.org/10.1007/s00484-024-02766-7

ORIGINAL PAPER

The development of an adaptive heat stress compensability classification applied to the United States

Gisel Guzman-Echavarria[1] · Ariane Middel[2,3] · Daniel J. Vecellio[4] · Jennifer Vanos[5]

Received: 16 April 2024 / Revised: 2 August 2024 / Accepted: 19 August 2024

Abstract

Traditional climate classification and weather typing systems are not designed to understand and prevent heat illness, or to design effective cooling strategies during extreme heat. Thus, we developed the Heat Stress Compensability Classification (HSCC) combining open-source historical weather data (2005–2020) with biophysical modeling of a standard human, in the sun or shade, during peak city-specific hot hours on the top 10th percentile hottest days in 96 U.S. cities. Four categories of uncompensable heat stress (UHS)—which can result in rising core temperature—were established based on the relative constraints of dry and evaporative heat exchanges for achieving heat balance in proportion to constant metabolic heat production (112Wm^{-2}). Results show that 88.7% of these peak-hot hours meet the UHS criterion, and 41% present a dry heat gain of 70 to 150Wm^{-2} while allowing a maximum evaporative loss between 90 and 140Wm^{-2}. Evaporative heat loss constraints dominate the eastern U.S. Dry heat gain was widespread, yet particularly high in the south and southwest. Full shade reduces UHS frequency to 7.6%, highlighting the importance of quality shade access and accounting for radiative load in heat stress assessments. Although there are five distinct categories (one compensable and four UHS), the HSCC is dynamic and customizable, providing actionable information on thermal variations within a given category. These variations depict the reason for UHS (e.g., limited evaporative cooling) and, thus, how to concentrate cooling efforts, particularly at the limits of physiological adaptability. Findings facilitate developing targeted criteria for heat stress reduction with potential global applications.

Keywords Heat Stress Compensability Classification (HSCC) · Extreme heat · Uncompensable Heat Stress · Climate Classification · Mean Radiant Temperature · Biophysical heat-exchange model

Introduction

Various classification or categorization systems are used to identify climate regions connected to vegetation and hydrology (Holdridge 1947; Köppen 1884; Thornthwaite 1948), building energy use (Bai et al. 2020; Walsh et al. 2017a, b), and various public health applications (Liss et al. 2014). These systems explain expected environmental conditions using select climate variables across a year/season (Gupta et al. 2023) and their effects on various human or natural systems. Climate classification systems guide regional building design by distributing spatial energy and water efficiency criteria, thus upholding indoor comfort. For the specific case of the United States (U.S.), based on the International Energy Conservation Code zoning, the Building America program updates climate zone designations (Antonopoulos et al. 2022; Lstiburek 2000). Yet, no system exists to express weather or climate

✉ Gisel Guzman-Echavarria
gguzma20@asu.edu

1 School of Geographical Sciences and Urban Planning, Arizona State University, P.O. Box 875302, Tempe, AZ 85287-5302, USA

2 School of Arts, Media and Engineering, Arizona State University, Tempe, AZ 85287-5802, USA

3 School of Computing and Augmented Intelligence, Arizona State University, Tempe, AZ 85287-8809, USA

4 Department of Geography/Geology, University of Nebraska at Omaha, Fairfax, NE 68182-0199, USA

5 School of Sustainability, Arizona State University, Tempe, AZ 85287-7904, USA

Published online: 16 September 2024

variables for environmental health applications, such as to analyze extreme heat by location identifing the environmental heat stress and associated physiological strain.

Extreme heat is a well-known and increasing physical hazard globally, with increased prevalence linked to climate change and urban growth (Perkins-Kirkpatrick and Lewis 2020), further challenging the ability to cope with anomalous heat extremes (Krayenhoff et al. 2018; Nazarian et al. 2022; Vecellio et al. 2023). Like other hazards, extreme heat events are described by intensity, scale, timing (*i.e.,* seasonally), and duration based on local climatology (e.g., see Table 1 in Barriopedro et al. 2023). Health impacts of heat are often recorded daily or across a heatwave, yet physiological effects from high heat exposure can occur on sub-daily and hourly time scales (Baldwin et al. 2024). These impacts will differ based on a person's exposure to temperature, humidity, sunlight, and airflow, as well as their activity levels and clothing. Moreover, research highlights that the physiological underpinnings of heat strain in a humid heat versus a dry heat differ (Foster et al. 2021, 2022a, 2022b; Vanos et al. 2023; Vecellio et al. 2022). Finally, heat impacts are more dangerous for certain groups of people, such as those more sensitive due to older age, lack of acclimatization, low fitness, medication usage, and/or co-morbidities (Ebi et al. 2021; Larose et al. 2013; Wolf et al. 2023).

Hence, climates can be classified not only by their impacts on environmental and built systems (Gupta et al. 2023) but also by their probable physiological effects on humans, supporting an improved understanding of health outcomes and suitable behaviors by sub-population, time of year, location, intensity, etc. For example, specific behavioral adaptations for heat relief (e.g., fan use) across varying climates and cultures require explicitly characterizing the thermal environment and exposure for particular populations (Manu et al. 2016; Morris et al. 2021). Such behavioral adaptations are increasingly necessary when the body cannot physiologically cope with heat (i.e., under uncompensable heat stress—UHS). Nevertheless, few studies differentiate "types" of heat geographically applied to people's health and potential physiological responses. Weather typing systems, such as the Spatial Synoptic Classification (SSC) (Sheridan 2002) and the Global Weather Typing Classification (Lee 2020), categorize daily weather by temperature and humidity, yet are not applied to individual physiology. In the SSC, the "plus" categories (or warmer than normal) have even been added to the tropical categories to delineate "extreme" conditions (Sheridan 2002). The spatiotemporal relativity of these systems provides indirect measures of seasonal and regional acclimatization for localized populations during extreme events, thus helping to describe weather and health interactions (e.g., Greene et al. 2011, Vanos et al. 2015, and Fonseca-Rodríguez et al. 2023). However, such studies are more epidemiological in nature, and the classification systems were not created with any direct physiological implications in mind.

Several heat or thermal stress indices have historically provided numerical representations of thermal stress using meteorological inputs (de Freitas and Grigorieva 2015, 2017; Ioannou et al. 2022). Yet many metrics are static in their application over space and time and do not allow for the inclusion of personal attributes complexities (as outlined in Grundstein and Vanos (2020), Guzman-Echavarria et al. (2022) and Simpson (2024)). Further, those indices do not provide information on reasons for heat loss restriction from the body and thus do not support the implementation of effective cooling strategies. Instead, a biophysical human heat exchange approach allows the determination of UHS by partitioning the different heat avenues to and from the body. UHS is a condition that occurs when the body's evaporative cooling requirements cannot be supported due to environmental or other factors (including low sweat production) impeding the body's ability to cool (Bouchama et al. 2022; Leon & Bouchama 2015). Importantly, this approach can be applied across diverse subpopulations and climates, both indoors and outdoors.

Here, we introduce a new classification system—the Heat Stress Compensability Classification (HSCC)—a weather-based characterization of extreme heat using the biophysical heat exchange principles underpinning UHS. The system is applied to 96 cities in the U.S. during the peak hot hours for the city-specific hottest 10% of days, as defined by the 90th percentiles exceedance of daily maximums of dry-bulb (T_{db}) and wet-bulb (T_w) temperatures from 2005–2020. The classification goes beyond a unidimensional "yes/no" for extreme heat by discriminating between different types of "hot days" based on the factors contributing to UHS. Therefore, this approach serves as a bridge, translating extreme heat exposure into actionable knowledge by identifying the primary causes of unsafe heat gain leading to UHS (such as high humidity or excessive radiative load) and providing direct guidance to minimize the risk of people reaching a non-compensable state.

Materials and methods

In this study, we developed and applied a UHS classification using open-source long-term weather data from 96 U.S. cities. We categorized the hottest hours of the 10% hottest days as defined by both T_{db} and T_w between 2005 and 2020 for a person with body characteristics equivalent to the Universal Thermal Climate Index (UTCI) assumptions (details in "Physiological details for categorization application" section) while sun-exposed or in the shade. The cities were first selected to capture the most populated metropolitan areas in the U.S. (> 1 M population) and later based on nationwide geographical

coverage. See Table S1 and Figure S1 for city metadata. The methods used in this study are divided into three main steps: data preprocessing, data filtering (i.e., subsetting) to apply the categorization, and the HSCC categorization itself.

Climatic data preprocessing

Inputs of T_{db}, atmospheric moisture (P_v, water vapor pressure), wind speed (w_s), and mean radiant temperature (T_{MRT}) reaching an individual must be known to discern if the exposure to that thermal environment leads to UHS and within what UHS category (Fig. 2). Additionally, we included T_w to identify hot days, as we are interested in the most oppressively hot conditions beyond T_{db} ("Hot days selection" section). Intending to use long-term weather records and freely available data, we combined airport weather station data and estimated T_{MRT} from modeled solar radiation (outlined below). T_{db}, relative humidity and atmospheric pressure were taken from HadISD.3.3.0-global sub-daily station dataset version v331_202301p (Dunn 2019), available at https://www.metoffice.gov.uk/hadobs/hadisd/. These values were used to estimate T_w with the Davies-Jones method (Davies-Jones 2008) and P_v as our humidity metric (Baldwin et al. 2024). We assumed a constant wind speed of 0.3 m/s to isolate differences in UHS from temperature, humidity, and solar radiation. Future work will assess the sensitivity of UHS upon changing wind speeds (e.g., Foster et al. (2022a, b); Morris et al. (2021)).

Global horizontal irradiation (*GHI*), direct normal irradiation (*DNI*), and diffuse horizontal irradiation (*DHI*) were obtained from the National Solar Radiation Database (NSRDB) (Sengupta et al. 2018), given that standard weather stations do not provide solar radiation or T_{MRT} in their records. NSRDB dataset is obtained from satellite-derived atmospheric and land surface properties using NREL's Physical Solar Model (PSM). We used the PSM V3.1 (4 × 4 km grid) version available at https://developer.nrel.gov/docs/solar/nsrdb/psm3-download/.

Mean radiant temperature estimation

We calculated T_{MRT} assuming that estimates will be representative of an open space with no close obstacles (sky view factor = 1) over a flat weathered concrete surface with albedo $\alpha = 0.186$, similar to the concrete roof surface in Vanos et al. (2021) and emissivity $\varepsilon_g = 0.92$, like the C002 material in Kotthaus et al. (2014). T_{MRT} estimates were obtained from a mean radiant flux density approach as a weighted combination of 6-directional short- and long-wave radiant fluxes to a standing man using the Stefan-Boltzmann law (Höppe 1994; VID 1994) (VID 1994) adapted from Middel et al. (2023).

Appendix A describes the process to estimate T_{MRT} and Figure S2 displays the model performance of the radiative flux budget and the surface energy balance. This method used the NSRDB data, sun elevation, and azimuth angle for shortwave radiation estimates. In this model, the incoming long-wave radiation ($L_{\downarrow}$) applies the Stefan-Boltzmann law using T_{db}, P_v, shortwave estimates, and Prata's (1996) sky emissivity equation. For outgoing long-wave radiation, the Stefan-Boltzmann law and a surface energy balance solution for urban areas were used (Oke et al. 2017), in which the net heat storage (or ground soil flux in this case) was calculated using the Objective Hysteresis Model (Grimmond et al. 1991), assuming coefficients for concrete urban facets (e.g., walls, ground) (Asaeda and Ca 1993). In that approach, the surface temperature was derived from the energy heat balance at urban facets (i.e., road), taking a bulk approach.

The estimation method for T_{MRT} was calibrated using observations from Vanos et al. (2021) in Tempe, Arizona, U.S. (33.426°N, 111.940°W) from Aug 21st through Nov 8th, 2016, with predominantly low cloud cover, obtaining a T_{MRT} RMSE of 2.95°C. Errors in $L_{\downarrow}$ data are similar to those reported by Lindberg et al. (2008) with a RMSE error of 23.15 Wm^{-2} (Figure S2). However, due to the sensible heat flux overestimation caused by assuming clear sky conditions, T_{MRT} estimates are expected to be slightly higher than otherwise observed.

Hot days selection

To select the top 10% of hottest days in each city, we chose not to rely merely upon T_{db} because the cause of heat stress would be biased towards dry-weather cities (Morris et al. 2021). Therefore, we include T_w to ensure that we also incorporate input data from environments that lead to high heat stress in humid places. To select the most oppressive conditions for T_{db} and T_w separately (Fig. 1a and b, respectively), we aggregated the hourly data to daily data based on the maximum daily temperature value (T_{max}) for both metrics. Then, the hottest day samples for each city were determined based on the exceedance of the 90th percentile. The final dataset thus represents the weather corresponding to the days and hours from the joined sample of T_{db} and T_w (Fig. 1c), where repeated temporal records were included only once. Note that HSCC in the following steps was applied only for the weather during those hottest hours of the day. Figure S3 displays the variability of T_{db}, T_w, relative humidity, P_v, and T_{MRT} per city during the top 10% of hottest days.

Heat stress categorization

The rationale behind the different types of uncompensable heat stress

From a biophysical perspective, heat stress is compensable when the heat produced by the body's metabolic processes and gained from the environment is ultimately offset through

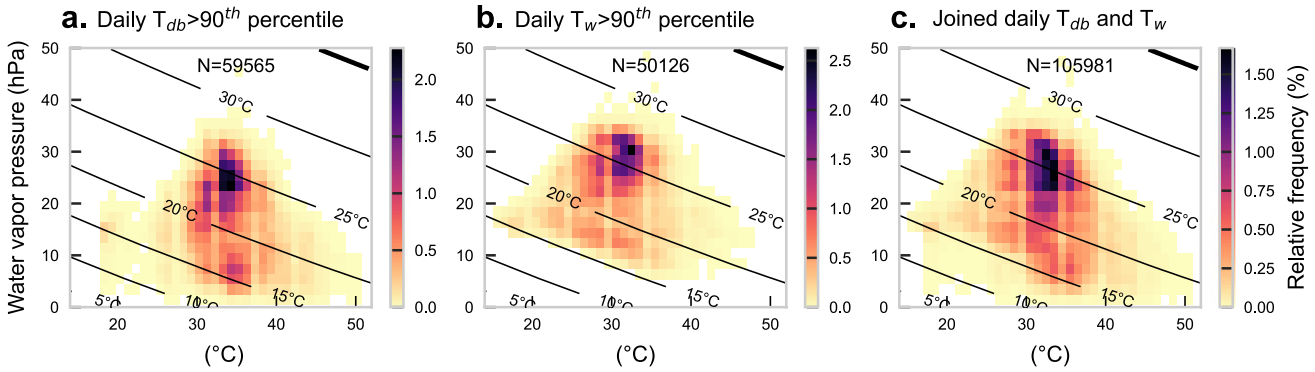

Fig. 1 The resulting temperature sample from all 96 cities with the associated time-matching moisture levels during the daily T_{max} above the 90th percentile for (**a**) T_{db}, (**b**) T_w, and (**c**) the joined dataset of (a) and (b). For the number of observations in the joined dataset, if a T_{db} and T_w observation matches in day and time of day, it is counted once. If the same day is identified but T_{db} and T_w peak at different times, those observations are treated separately

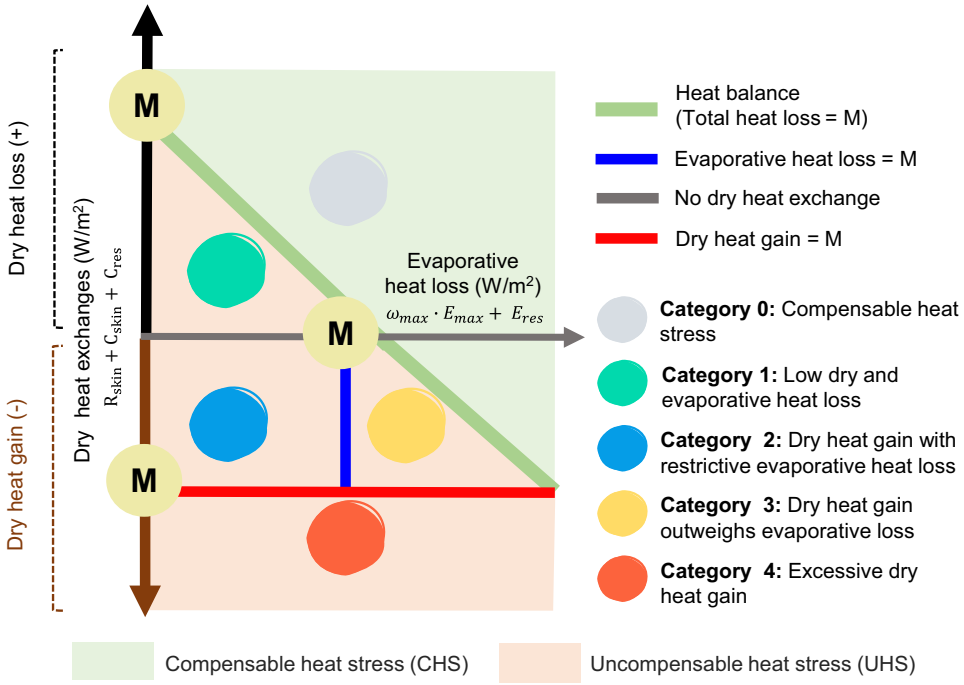

Fig. 2 Schema of compensable vs uncompensable heat stress (UHS) and different categories of UHS based on the relative contributions of dry $(R_{skin} + C_{skin} + C_{res})$ and evaporative heat exchanges $(\omega_{max} \cdot E_{max} + E_{res})$ in proportion to a fixed value of internal metabolic heat production (M). The green line divides compensable (light green area) from uncompensable heat stress (light red area); the grey line indicates the limit between dry heat loss or gain; the blue line divides the area where evaporative heat loss is enough to dissipate metabolic heat; and the red line delineates when dry heat gain is higher than metabolic heat production

increased evaporative heat loss (and, to a lesser extent, dry heat loss if $T_{sk} > T_{db}$), enabling the human body to keep a stable internal temperature (Cramer et al. 2022). This compensability can be expressed using human–environment heat exchange models comparing the rate of evaporative heat loss required for heat balance (E_{req}) and the maximum capacity for evaporative heat loss given a set of environmental and clothing settings (E_{max}). Thus, when $E_{req} < E_{max}$, one experiences compensable heat stress (CHS), and vice versa, when $E_{req} > E_{max}$, UHS is experienced. E_{req} can be expressed using the human heat balance equation (Eq. 1) assuming null heat storage and negligible mechanical work (*i.e.,* the energy transferred to a force) and conductive heat exchange (i.e., $S, K, W_k = 0$ W):

$$E_{req} = M - R_{skin} - C_{skin} - C_{res} - E_{res} \text{ (W, or W}^{-2} \text{ if divided by body surface area)} \quad (1)$$

The assumption of negligible $W_k = 0$ is used to express that internal metabolic heat production (H_{prod}) is equivalent to metabolic rate (M). R_{skin} and C_{skin} represent rates of dry heat exchange by radiation and convection through the skin and can be negative or positive depending on whether there is heat loss or gain. That heat gain/loss relies on the gradient between the skin temperature (T_{sk}) and operative temperature t_0 (*i.e.,* a temperature value that combines the effect of T_{db} and radiant heat over a surface), in °C.

$$R_{skin} + C_{skin} = \frac{(T_{sk} - t_0)}{\left(R_{cl} + \frac{1}{(h_{c+r}) * f_{cl}}\right)} \ (\mathrm{Wm}^{-2}) \tag{2}$$

R_{cl} is the dry heat transfer resistance of clothing (m^2 °C W^{-1}), h_{c+r} is the combined convective heat transfer coefficient ($Wm^{2}°C^{-1}$)—or the sum of the convective (h_c) and radiative (h_r) heat transfer coefficients for airflow around humans—and f_{cl} is the clothing area factor. For equations t_0, R_{cl}, h_c, h_r, f_{cl}, and A_d, see Cramer and Jay (2019) and Vanos et al. (2023). T_{sk} is held constant at 36°C (Parsons 2014).

In Eq. 1, C_{res} and E_{res} represent the convective and evaporative heat exchange in the respiratory tract:

$$C_{res} = 0.0014 \cdot M\left(34 - T_{air}\right) \ (\mathrm{Wm}^{-2}) \tag{3}$$

$$E_{res} = 0.0173 \cdot M(5.87 - P_v) \ (\mathrm{Wm}^{-2}) \tag{4}$$

Conversely, E_{max} accounts for environmental and clothing restrictions to body heat loss via sweat evaporation (Eq. 5). To consider the physiological capacity to wet the skin and distribute sweat across the skin surface in humid environments, E_{max} is constrained to the maximum skin wettedness (ω_{max}). ω_{max} represents the maximum percentage of the body that can be covered by sweat, ranging from 0.85 for fully heat-acclimatized to 0.65 for not heat-acclimatized or individuals older than 65 years (Candas et al. 1979; Morris et al. 2021). In this application of the HSCC, we used an intermediate value of 0.7.

$$E_{max_{env}} = \frac{(P_{sk,sat} - P_v)}{R_{e,cl} + \frac{1}{h_e * f_{cl}}} \ (\mathrm{Wm})^{-2} \tag{5}$$

$P_{sk_{sat}}$ is the water vapor pressure at the skin surface when saturated with sweat (kPa), $R_{e,cl}$ is the evaporative resistance of clothing (m^2kPa W^{-1}), and h_e is the evaporative heat transfer coefficient (Wm^{-2} kPa^{-1}). The $P_{sk_{sat}}$ is calculated from T_{sk}. For the equation for h_e, see Cramer and Jay (2019).

Taking the heat compensability limit when E_{req} equals the body's capacity to lose heat via sweat evaporation (i.e., $E_{req} = \omega_{max} \cdot E_{max_{env}}$), we replace terms from Eqs. 1 and 5 and rearrange the equation as a function of metabolic heat (Eq. 6). Hence, from Eq. 6, the physiological problem of heat compensability can be seen as the possibility of overcoming the internal heat production by achieving enough heat loss while considering the combined environmental, clothing, and physical effect on heat balance. In turn, this formulation allows us to group heat avenues into dry and evaporative heat balance components in proportion to a constant value of M, which is the foundation for categorizing the different types of UHS, explained below.

$$M = \left(\omega_{max} \cdot E_{max} + E_{res}\right) + \left(R_{skin} + C_{skin} + C_{res}\right) \ (\mathrm{Wm}^{-2}) \tag{6}$$

Having the compensability/uncompensability limit at a fixed level of M allows us to describe extreme heat using UHS explained in terms of the main constraints in heat loss by environmental conditions (i.e., constraints due to evaporative heat loss, dry heat loss, or both). Graphically, this problem is shown in Fig. 2.

Thus, the five categories of HSCC classification were established based on the relative contributions of dry and evaporative heat exchanges in proportion to the internal metabolic heat production needed to dissipate, as follows:

Category 0 Compensable heat stress (CHS): Heat stress is compensable because total heat loss is equal to or greater than the metabolic heat production ($M < \left(\omega_{max} \cdot E_{max} + E_{res}\right) + \left(R_{skin} + C_{skin} + C_{res}\right)$). All conditions close to heat balance are at the edge of the transition from CHS to UHS, exerting high heat stress on people.

Category 1 Low dry and evaporative heat losses: UHS occurs because evaporative heat loss is not possible $\left(\omega_{max} \cdot E_{max} + E_{res} < M\right)$, and dry heat loss is small $\left(0 < R_{skin} + C_{skin} + C_{res} < M\right)$. This condition typically occurs in environments with high humidity (moisture) and air temperatures.

Category 2 Dry heat gain with restricted evaporative heat loss: UHS occurs because evaporative heat loss is not possible $\left(\omega_{max} \cdot E_{max} + E_{res} < M\right)$, and the body gains heat via convection and radiation $\left(-M < R_{skin} + C_{skin} + C_{res} < 0\right)$. This condition typically occurs in an environment with high humidity, air temperature, and solar radiation.

Category 3 Dry heat gain outweighs evaporative loss: UHS occurs despite possible evaporative heat loss $\left(M < \omega_{max} \cdot E_{max} + E_{res}\right)$, but the heat gain via convection and radiation outweighs the evaporative heat loss $\left(\left[\omega_{max} \cdot E_{max} + E_{res}\right] + \left[R_{skin} + C_{skin} + C_{res}\right] < M\right)$. This condition typically occurs in drier environments with high air temperatures and solar radiation.

Category 4 Excessive dry heat gain: UHS occurs due to excessive heat gain (greater than M) $\left(R_{skin} + C_{skin} + C_{res} < -M\right)$, whether or not evaporative heat loss is possible. This condition is common in arid environments with exceedingly high air temperatures and intense solar radiation. This category is the most severe in this classification, adding that sweat rate limits do not restrain evaporative loss, as in Vanos et al. (2023).

The HSCC system reports three types of results. *First,* a binary outcome describes whether heat stress is compensable or uncompensable (Fig. 3a). *Second*, heat stress typology is defined when heat is uncompensable (Fig. 3b and c, Table S3). *Third*, within UHS, we can directly compare dry against evaporative heat losses, as summarized in the 2D histogram of the human heat balance (Fig. 5).

This third report type delineates the reasons for UHS grouping observations according to their potential evaporative heat flux $\left(\omega_{max} \cdot E_{max} + E_{res}\right)$ on the x-axis and dry heat

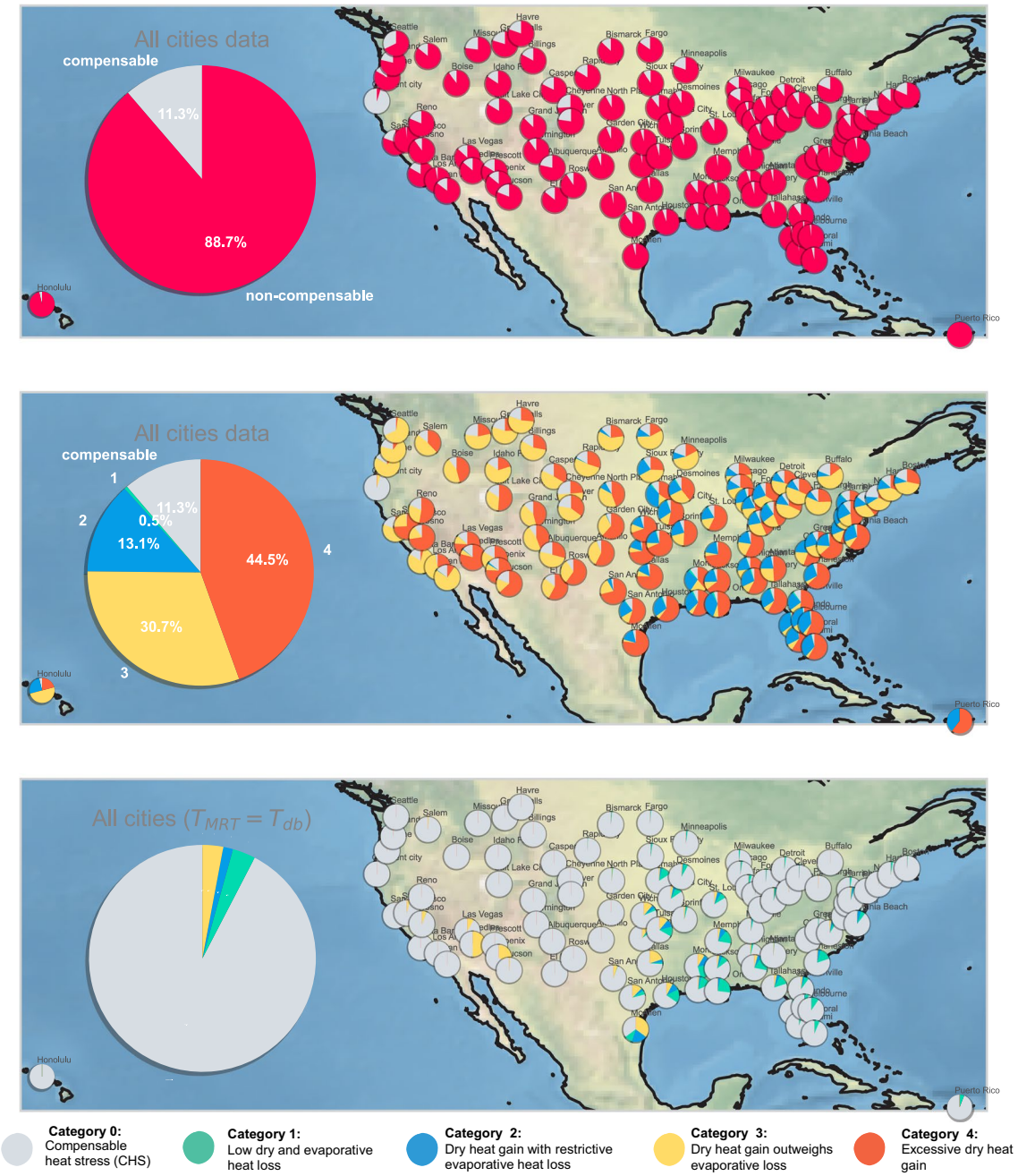

Fig. 3 Proportion of days with compensable and uncompensable heat stress from the top 10th percentile of hottest days in 96 U.S. cities based on the peak T_{db} and T_w from 2005–2020. (**a**) Displays results as a binary compensable-uncompensable heat stress outcome, while (b and c) detail the type of UHS (Categories 1 to 4). For (**b**) the categorization is applied for heat exposures with an estimated T_{MRT} as a sun-exposed condition, whereas in (**c**) the results are applied for a person entirely shaded ($T_{MRT} = T_{db}$). An interactive version of the (b) plot is available in https://zenodo.org/records/10899894, along with 2D histograms (as in Fig. 5) with heat balance results for each city. Input data for these graphics are in Table S3

exchange (loss or gain) $\left(R_{skin}+C_{skin}+C_{res}\right)$ on the y-axis, both in Wm^{-2}. Given the fixed value of metabolic heat production, a diagonal line (Fig. 5) expresses heat balance (total heat loss = metabolic internal heat). In the same plots, the grey line indicates a null dry heat exchange $\left(R_{skin}+C_{skin}+C_{res}=0\right)$, the red line indicates where dry heat gain equals metabolic heat production $\left(R_{skin}+C_{skin}+C_{res}=-M\right)$, and the blue line separates conditions where evaporative heat loss could surpass metabolic heat production $\left(\omega_{max}\cdot E_{max}+E_{res}=M\right)$. Note that the absolute values of heat flux thresholds from all categories depend on metabolic heat production.

Physiological details for categorization application

To apply the HSCC, we must specify an individual's personal characteristics. For this initial iteration of the HSCC, we adopt a UTCI operational set-up characteristics (Bröde et al. 2012) representing a healthy "average" adult male walking with a speed of 4 $km.h^{-1}$ (1.1 ms^{-1}) at M = 2.3MET, wearing light clothes, with a mass of 73.4 kg and height of $1.85m^2$ (Fiala et al. 2012), resulting in M=206.8W or $111.79Wm^{-2}$ after a mass-based factor conversion. The human–environment heat exchange estimations were done using the PyHHB module (Guzman-Echavarria and Vanos 2023) and UTCI adaptative clothing scheme capped at a minimum of 0.31clo (Havenith et al. 2012; Vanos et al. 2012). Future work with this categorization can use multiple physiological settings.

Results

Results display the application of the HSCC during extreme heat conditions for 96 U.S. cities and demonstrate the importance of accounting for the radiative load in biometeorological applications for heat stress. In addition, we provide examples of various reporting methods possible with this system, highlighting the types of thermal environments captured by each category given the personal profile used (which can be customized in further applications).

Input data: weather during peak heat hours on the top 10% of warmest days

The environmental input data for the classification comprises 105,981 hourly observations during the top 10% of the warmest days of each city based on T_{db} and T_w daily maximums. T_{db} exhibits a median (and interquartile range: IQR) of 32.8°C (30.0–34.6°C), ranging from a minimum of 15.0 to a maximum of 50.1°C. The mean T_{MRT} is 65.9°C (60–70.1°C), ranging from 10.4 to 91.1°C, while P_v has a mean of 21.3 hPa (14.5–26.7 hPa), ranging from 0.5 to 47.7 hPa. Relative humidity has a median of 44.6 (29.2–58.0%), ranging from 0 to 100%. The majority of peak the hottest hours in each city occurred between June and August (maximum in July) from 2:00–3:00 pm local time, except San Juan-PR, Honolulu-HI, Miami-FL, Melbourne-FL, and some cities along the Pacific Coast where peak heat hours occurred mostly between 12:00–2:00 pm. The hottest hours of occurrence from those time frames along the Pacific Coast is mainly related to high T_w. Appendix B in the Supplementary Material describes weather variability between (Figure S3) and within all cities (Figure S4, Table S2).

HSCC Heat Stress Categorization Results

We found that 88.7% of input data met the UHS criterion (Fig. 3a), meaning that at least during ~ 94,000 days weighted by city, people might be exposed to conditions in which they had to engage in cool-seeking behavior to keep safe from the regional heat. However, there is substantial heterogeneity in UHS typology across the cities studied (Fig. 3b). Only nine cities have more than 20% of observations within CHS, mainly in the northern U.S., while 26 present UHS conditions > 95% of the time. The higher UHS frequencies are found in San Juan (99.87%), Stockton-CA (93.37%), Melbourne-FL (98.13%), Orlando-FL (98.1%), and Cape Coral-FL (98%).

Figure 3b shows the categorization results grouping the extreme heat values for all 96 cities. **Category 1 (low dry and evaporative heat losses)** was assigned to only 0.46% of the data, where only three cities reported > 2% frequency (*i.e.,* Monroe-MO, New Orleans-LA, and Jacksonville-FL). **Category 2 (Dry heat gain with restrictive evaporative heat loss)** accounts for 13.1% of data, with 36 cities, all concentrated in the east, having more than 20% of observations. San Juan (Fig. 5c), Omaha-NE, Melbourne, New Orleans (Fig. 5f) and Miami (5e) have the highest frequency of Category 2 (> 34% observations), all presenting low evaporative heat loss capacity values (< M) during extreme heat. **Category 3 (dry heat gain outweighs evaporative loss)** represents 30.7% of the data, with higher frequencies found in cities along the Pacific coast. For example, Santa Barbara-CA, San Francisco-CA, and San Diego-CA present > 75% of observations in Category 3. **Category 4 (Excessive dry heat gain)** is found in 44.5% of the cities, being the most frequent category in the sample, with five having > 75% observations in this category (Needles-CA, Mc Allen-TX, Las Vegas-NV, Phoenix-AZ, and Dallas-TX) and 43 cities with > 50%.

Weather conditions and personal heat loads by category

This section describes the weather conditions captured within each category (Fig. 4d-f), as well as heat loads and heat compensability in terms of the required skin wettedness (ω_{req}) to achieve heat balance (Fig. 4a-c).

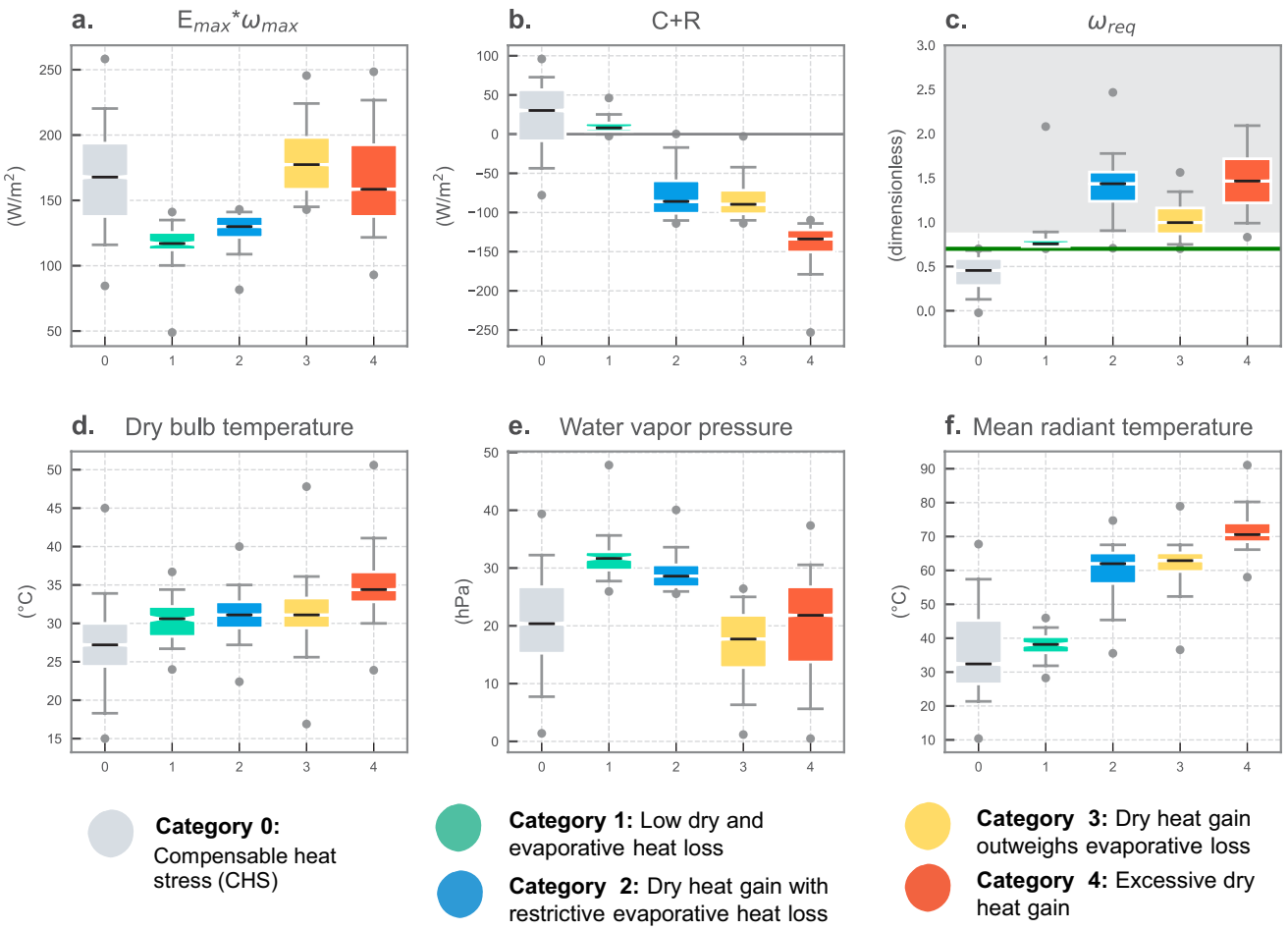

Fig. 4 Variability per category of (**a**) potential evaporative heat loss, (**b**) dry heat exchanges (positive = loss, negative = gain, grey line: null heat dry exchanges), (**c**) required skin wettedness (ω_{req}) to achieve heat balance (green line = ω_{max}, the grey background indicates ω_{req} values above 1 —or 100% of skin surface— which are not physically feasible), (**d**) T_{db}, (**e**) V_p, and (**f**) T_{MRT}. Boxes indicate IQR with the median marked by a black inside line, and whiskers displays the 5th and 95th percentile. Minimum and maximum values are shown as points. Median and IQR from (a-f) subplots are reported in Table S4 in the Supplemental Material

Category 0 has wider variations due to the CHS possibility under thermal environments that lead to either high evaporative heat loss (dry environments) or higher dry heat loss (colder temperatures) (see Table S4). As a result, possible dry and evaporative heat fluxes were the widest compared to all categories (a median (IQR) of 30.2Wm^{-2} (-8.53, 56.67Wm^{-2}) for dry and 167.8Wm^{-2} (137.71, 193.82Wm^{-2}) for evaporative heat fluxes). A slight variation is found in the weather parameters in **Category 1**, shown by the smaller IQRs in Fig. 5. Although UHS is in this category, the median ω_{req} (0.76) is the lowest (hence, this is the least stressful category). **Category 2** presents characteristics similar to **Category 1**, yet with lower moisture levels and considerably higher T_{MRT} (23.8°C greater based on median values). The higher moisture and T_{MRT} are largely responsible for almost double ω_{req} (1.44) compared to category 1. The dry heat gain in **Category 3** outweighs the evaporative heat loss yet does not exceed metabolic heat production, resulting in a median ω_{req} of ~ 1.0. **Category 4** presents the highest values of T_{db}, T_{MRT}, and GHI, yet a wide variation in moisture levels; hence, this category brings the possible occurrence of both very hot and humid heat stress. As a result, the ranges of possible dry heat gain with a median (IQR) of -133.82Wm^{-2} (-150.5, -122.23Wm^{-2}) and the highest median ω_{max} (1.47), thus being the most severe HSCC category.

Overall, results from Categories 1–4 can be interpreted as the amount of cooling that is possible for a group of sun-exposed people with average body characteristics and clothing (i.e., UTCI profile) to keep them in CHS (Fig. 5a). Beyond observations being categorized, the 2D histogram shows that ~ 41% of the hottest hours of the 10% hottest days from 2005–2020 exerted dry heat gain from 70 to 150Wm^{-2}, allowing a maximum evaporative loss between 90 and 140Wm^{-2}. Thus, heat gain must be limited to these thresholds while enhancing the evaporative heat flux to keep heat stress compensable.

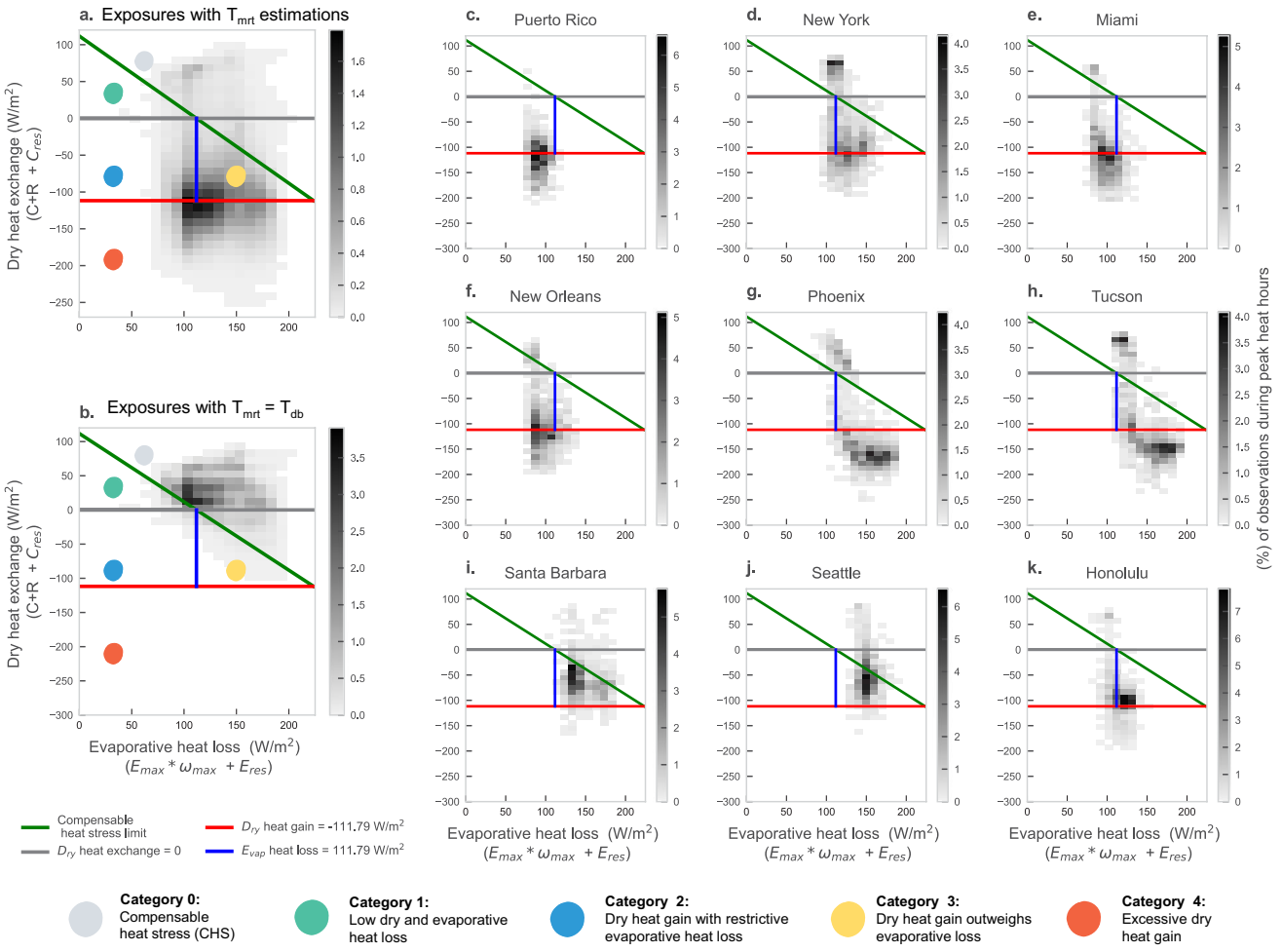

Fig. 5 2D histograms displaying the relative frequency of observations disaggregated into bins of 10 Wm^{-2}, indicating the relative contributions of evaporative (x-axis) and dry (y-axis) heat exchanges in proportion to a fixed value of internal metabolic heat production ($M = 111.8 Wm^{-2}$). Data are provided for all input data (**a**, **b**) and selected city examples: San Juan (**c**), New York (**d**), Miami (**e**), New Orleans (**f**), Phoenix (**g**), Tucson (**h**), Santa Barbara (**i**), Seattle (**j**), and Honolulu (**k**). In (a) heat fluxes represent heat exposures with estimated T_{MRT} as sun-exposed conditions, and (b) heat exposures for a person who is fully shaded ($T_{MRT} = T_{db}$). The histogram plots for all cities are shown in the interactive version of Fig. 3 in https://zenodo.org/records/10899894

Within-city variability in heat loads

As depicted in "HSCC Heat Stress Categorization Results" section, a given city can present different types of (or reasons for) UHS based on high heat that arises due to diverse synoptic genesis. This section presents the possible heat loads on a person during extreme heat in U.S. cities with the highest air temperature combined with extremely high or low moisture levels, as well as some with the coolest conditions (see Fig. 5). We also present results from cities with the narrowest and widest variability in T_{db}, T_{MRT} and P_v (Appendix B).

San Juan (Fig. 5c), located in the north of Puerto Rico with a tropical rainforest climate (Köppen *Af* class), has the highest frequency of UHS, demonstrating high dry heat gains (up to ~ $220 Wm^{-2}$) in combination with low evaporative heat losses (~ 70–$110 Wm^{-2}$). Honolulu (Fig. 5k) (with a similar latitude as San Juan yet a semi-arid climate (Köppen *BSh*) has most of its extreme heat days in category 3, where dry heat gain outweighs evaporative heat loss (around 120–$140 Wm^{-2}$).

In the East, New York (Fig. 5d) displays highly heterogeneous UHS behavior (spread among numerous categories with no distinct clustering), which differs from Florida cities and New Orleans, in which dry heat gain was often around $100 Wm^{-2}$ (up to 200 Wm^{-2}) yet with low and narrow evaporative heat loss variations around 80 to $100 Wm^{-2}$.

Cities located in the South and Southwest (highest T_{db} and T_{MRT}) reveal the highest dry heat gains (~ $150 Wm^{-2}$), reaching values of $240 Wm^{-2}$ (see Phoenix and Tucson in Fig. 5). Arizona cities also display the greatest values in maximum possible evaporative heat losses (up to ~ $200 Wm^{-2}$), which could even demand nonfeasible

sweat rates for people with impaired sweating. Another aspect relevant in Southwest cities is the apparent bimodality in UHS, with high frequency at lower evaporative heat fluxes values (100-120Wm^{-2}) that should be associated with T_w inclusion in a hot day selection and, therefore, summer monsoon days. Finally, the Pacific coast has more instances of CHS; when UHS occurs, it is dominated by high values of evaporative heat loss and low dry heat gain (< ~ 150Wm^{-2}) when within Category 4 (Fig. 5i-j).

The role of radiative heat load and uncompensable heat stress

The inclusion of radiant load in heat stress was tested by assuming a change from the T_{MRT} estimated initially (open, sun-exposed) versus full shade, wherein $T_{MRT} = T_{db}$. While maintaining maximum evaporative loss between 90 and 140W/m^2, the overall effect of shade shifts the dry heat gain into possible heat loss. This shift results in low dry heat loss values from 5 to 50W/m^2 (Fig. 5b) ~ 40% of the time, which could be enhanced with increased airflow to support further convective heat loss. This radiative change represents a reduction in the frequency of UHS to 7.62% (Figs. 3c and 5b) across all input data (comprised of 3.27% in Category 1, 1.39% in Category 2, 2.96% in Category 3, and 0% in Category 4).

Discussion

We report on the development and application of the Heat Stress Compensability Classification (HSCC), which combines historical weather data with biophysical modeling during peak city-specific hot hours, as defined by the 90th percentiles of daily maximums for T_{db} and T_w over 15 years in 96 U.S. cities. The classification uniquely uses fundamental principles from thermal physiology and human biophysics to determine the main avenues for heat gain and loss to describe UHS on extreme heat days. In the long term, this knowledge can support cooling procedures by category based on the heat flux values that best achieve heat balance, adopting a similar standpoint as in building sciences to estimate cooling loads (Mao et al. 2018).

The HSCC is the first climate-based classification system to focus on human heat health from a person-centric approach because, unlike other systems and heat stress related metrics (like the UTCI itself), it provides actionable data to support decisions on personal heat-specific adaptations. Having a strong focus on human physiology, the HSCC can act as a baseline to mitigate and adapt to extreme temperatures. The HSCC is dynamic and customizable, allowing for more than just a categorical description of environmental conditions, but information on thermal variations within a given category that informs users about the reason for UHS (or dangerous heat) and, thus, how to change personal cooling strategies or behaviors. The HSCC approach also overcomes drawbacks of common bioclimatic models wherein solar radiation is not considered (e.g., NOAA's Heat Index, Humidex, T_w), and its flexibility allows for future work adjusting metabolic heat loads along with environmental factors (e.g., airflow).

Insights from HSCC to mitigate UHS

It is well-known that seeking shade is one of the top forms of human agency for reducing heat exposure through behavioral adaptation (de Freitas 2015; Horton et al. 2021). In hot conditions, minimizing radiative heat sources is crucial to reduce heat stress, as demonstrated in this research ("The role of radiative heat load and uncompensable heat stress" section). For the personal characteristics simulated in this study, exposure to UHS conditions would occur only during 7.6% of days if people stayed indoors or in the shade, as opposed to 88.7% of days when solar radiation exposure is considered. Assuming $T_{MRT} = T_{db}$ implies no radiant thermal load contribution, which is the most favorable scenario within shade effectiveness. However, some people may not have the choice (e.g., working outdoors) or the ability to seek shade/indoors. For example, in Phoenix (Fig. 5f), on an average peak heat summer hour (3:30 pm), dry heat gain is around ~ 153.5Wm^{-2}. If a person stands outdoors in the shade (no change of T_{db}), under a tree or a lightweight engineered structure, the ΔT_{mrt} will be -22°C (Middel et al. 2021); hence, the dry heat gain could be reduced to 66Wm^{-2}. That reduction could be even bigger and reach 42.1Wm^{-2}, if the shade is provided by an urban form/building (ΔT_{mrt} = -28°C, Middel et al. (2021)). However, in such cases, with possible evaporative losses between 120 and 180Wm^{-2}, heat stress will be closer to, but not quite compensable, requiring additional cooling actions (more than only shade) to keep people safe.

Several optimal low-cost personal cooling strategies are being tested to overcome the dependency on mechanical cooling (air conditioning). For detailed information on the benefits of individual cooling strategies, see Jay et al. (2021). Under non-extreme heat conditions, when T_{db} is less than skin temperature, using fans simultaneously enhances evaporative and convective heat fluxes. However, fan impact is strongly determined by air temperature and humidity. Recent empirical and modeling studies have provided critical insight into the optimal conditions for fan use across different populations and climates (Foster et al. 2022a, b; Morris et al. 2021;

Ravanelli et al. 2017). Within the HSCC system, it is implicit that beyond moisture levels linked to evaporative possible heat losses, the cooling suggestions (e.g., cooling amount) per category will vary according to the magnitude of dry heat exchanges and the metabolic load of the chosen sub-population-group (see Table 1).

Future opportunities for use

Although this initial HSCC application is delineated for U.S. cities and only one set of personal characteristics, the method can be replicated using any set of weather observations, physiological measurements, and metabolic

Table 1 Insight from this first HSCC application for the different categories and appropriate heat strain mitigation strategies beyond air conditioning. Note that the evidence stated here comes from both empirical and theoretical studies, and that strategies that might work as heat stress relief upon compensable heat stress might only work for the delay or short relief of heat strain, and thus require further cooling for keeping people safe during long heat exposures

Category	Actions
For all categories	Moving out of direct sunlight significantly lessens overall heat load (see "The role of radiative heat load and uncompensable heat stress" section) and should be the first action taken. Regardless of humidity and clothing, if air temperature ≤ 30°C at moderate exercise, fans will increase the benefits from convective heat loss (Foster et al. 2022a, b), although their effectiveness can extend at rest to 39 °C for young adults, 38°C for older, and 37°C for older adults taking anticholinergic medication (Morris et al. 2021). Other options include optimizing clothing to avoid heat gain while allowing sweat evaporation and conductive heat loss strategies to alleviate heat strain as cold water immersion of extremities (Khomenok et al. 2008) and the use of wet clothing (Cramer et al. 2020). Maintaining hydration is paramount to avoid additional strain across all categories
Category 0 (Compensable heat stress)	People are safely able to balance in the given conditions, yet if they are near the UHS limit, they might feel some thermal discomfort, thus people may actively seek various forms of cooling to keep safe and achieve thermal comfort
Category 1 (Low dry and evaporative heat losses)	In this least serious of categories, people can focus on increasing dry and evaporative heat losses, for example, by using fans (depending on the air temperature) and enhancing cooling by reducing clothing amount or insulation. Given low evaporative heat losses, it is suggested to avoid evaporative coolers or misting, particularly without additional airflow
Category 2 (Dry heat gain with restricted evaporative heat loss)	Actions should be taken to reduce or reverse dry heat gain. With high moisture in the air, even if T_{db} is around 36°C, the effect of fan use may help delay heart rate increase in the heat due to enhancing evaporative heat loss (Ravanelli et al. 2017). Cooling methods, like evaporative coolers or misters, that add moisture to the air should not be used, particularly without additional airflow
Category 3 (Dry heat gain outweighs evaporative loss)	Actions should be taken to reduce or reverse dry heat gain. For example, dousing skin and/or clothing with water; use misters, wet towels, and evaporative cooling. However, take caution with the use of fans without adding water to the skin/clothing as it can worsen dry heat gain (Foster et al. 2022a, b; Morris et al. 2021). For $T_{db} \geq 35$°C, fans are ineffective and potentially harmful when relative humidity is below 50% (Foster et al. 2022a, b). For example, At $T_{db} = 42$°C, 34 hPa, heat gain with fans increased ~ 70 Wm^{-2} (Ravanelli et al. 2017)
Category 4 (Excessive dry heat gain	This category exhibits the most severe heat stress with excessive dry heat gain and can become very dangerous rapidly if sweating shuts down. Here, heat strain mitigation might be most effective through misting, wet towels or shirts soaked in cold water and evaporative coolers, along with water dousing, given the high evaporative capacity of the air. However, combining strategies does not always maximize benefit. Empirical evidence in Cramer et al. (2020) for older adults at 42.4°C air temperature and 34.2% relative humidity shows that electric fan use coupled with a wet t-shirt exacerbates sweat losses without mitigating heat strain. Still, using only wet t-shirts without a fan instead alleviates sweat loss and heat strain. Overall, it is paramount to reverse dry heat gain to keep people safe and leverage the dry air for evaporation

workloads. The contextual findings for the United States are comparable to other hot and dry/humid locations. However, the within-city variability in many locations (e.g., coastal to inland regions; parks to open fields) demonstrates that one "type" (or category) of extreme heat does not define a place. Thus, heat mitigation strategies should be focused beyond the predominant type of climate and understand the variability across the summer season and a region.

Unlike other heat stress assessment methods, the practical utility of the HSCC stems from the limits of physiological adaptation. This categorization can evaluate diverse populations performing different activities to determine their customized HSCC. For example, empirical research reveals average dry heat exchanges from -1.5Wm^{-2} (humid experiments) to 76.9Wm^{-2} (dry experiments) in young, healthy adults without added radiant heat load in their limits to physiologically adapt to heat (Vecellio et al. 2022), which are plausible values in the current study (Fig. 5b). Also, current research has shown that environmental limits for heat adaptability decrease with moisture, activity, and age (Vecellio et al. 2022; Wolf et al. 2021; Tony Wolf et al. 2023). A calibrated HSCC by sub-population can give a more nuanced understanding (yet improved guidance) for different populations experiencing high heat loads. For example, modeling older adults (Vanos et al. 2023) and outdoor workers with a higher metabolic load would increase the frequency of UHS across the map. Overall, methods here can be expanded and improved based human-environmental heat exchange models in interdisciplinary research (see Table 3 in Vanos et al. (2023)).

The HSCC model and data from other scientific fields can be used as actionable information to guide extreme heat management, highlighting the role of personal cooling behavioral adaptations for safety in different indoor or outdoor contexts (Baniassadi et al. 2019; Jay et al. 2021; Larsen et al. 2022; Nazarian et al. 2022; Rempel et al. 2022; Samuelson et al. 2020). There are also potential applications in heat planning and disaster preparedness (e.g., compounding disasters, blackouts), design of infrastructure and public spaces to withstand extreme heat, and design, testing, and implementation of personal cooling strategies and clothing.

Limitations

The initial HSCC formulation has assumptions regarding the type of human (based on the UTCI-like average person), calm airflow, and unacclimatized humans, yet humans can adapt through physiological adjustments, such as increasing sweating capacity (Périard et al. 2015). Still, the model allows for size, shape, clothing, metabolic rate adjustments, variations for acclimatization, and for medications that affect sweat rate. The main limitation of this biophysical modeling approach are comprehensively outlined in Vanos et al. (2023) in Table 3, including holding skin temperature constant at 36°C or the skin wettedness values constant. As in Vanos et al. (2023), this method is able to represent exclusively heat strain that leads to hyperthermia and not to cardiovascular collapse or renal failure, acknowledging that heat stroke deaths are a fraction of total excess heat-related deaths (Ebi et al. 2021; MCDPH 2024; NYC Department of Health 2024). We also acknowledge that thermal environments at typical airport weather observation stations differ from people's daily experience (Kuras et al. 2017; Nazarian and Lee 2021). Yet, these stations provide long-term, consistent records and are helpful for city-wide, national-level surveillance applications, as well as baseline data to model mitigation strategies and heat in indoor environments.

Conclusions

This research introduces a novel classification system—the Heat Stress Compensability Classification (HSCC)—to describe uncompensable heat stress, which may result in rising core body temperature without altering one's heat stress conditions. The HSCC classification system is based on biophysical principles and thermal physiology, providing relevant information about the type of heat stress experienced by a person as a function of internal metabolic heat production. Using open-source historical weather data (2005–2020), this new classification system is successfully applied across 96 U.S. cities for the hottest hours in the hottest 10th of days (city-specific). In addition, this study introduces an approach to estimate T_{MRT} using weather station and radiation-modeled data to account for the importance of radiative load on heat stress.

Results from the HSCC are reported in three ways: 1) a binary compensable heat stress outcome, 2) uncompensable, describing the typology, and 3) disaggregating the category results within the human heat balance in a 2D histogram. Results show that 88.7% of the evaluated city-hours met the UHS criterion. Said differently, people may have been exposed to conditions in which they had to engage in cool-seeking behavior to keep safe (prevent rising core temperature) for ~ 94,000 h. Full shade reduced UHS frequency to 7.6%, highlighting the importance of quality shade access and including radiative load in heat stress assessments. The results from UHS categories help support decisions on changing a thermal environment. The practical utility of this system over other traditional methods (like UTCI or heat index) comes from its dynamic and customizable nature by 1) being adaptable to determine limits for various populations and target activities in heat stress assessments, and 2) providing graphical outputs showing how much heat needs to be mitigated to keep a specific population group in a thermally compensable condition based on their activity (e.g., a person walking in this application).

At the limits of physiological adaptability or survivability, these findings align with physiological theory and produce actionable information through the different ways of communicating the results and facilitating the development of targeted criteria for heat stress mitigation strategies with potential global applications. Finally, the HSCC demonstrates that heat mitigation strategies should, and can, be focused beyond viability for the predominant type of climate (place-specific) and account for the variability across the summer season and on people (time- and person-specific).

Supplementary Information The online version contains supplementary material available at https://doi.org/10.1007/s00484-024-02766-7.

Acknowledgements E.G. and JKV acknowledge funding from the National Science Foundation (NSF) Award #CMMI-2045663; AM also acknowledges funding from NSF Award #CMMI-1942805.

DJV acknowledges funding from the National Institute on Aging Grant T32 AG049676

We thank the climate modeling and research groups of HadISD and NSRDB for producing and making available their datasets. Data analysis and visualization code was developed using Python 3.8.8 and authors thank the teams behind this open-source project, as well as NumPy, Matplotlib, Seaborn, Pandas, Folium, and Cartopy developers.

Data Availability The intermediate data generated for this HSCC application is available from the corresponding author upon reasonable request. In the supplemental material is the input data for the Figure 3. The Appendix A python code (Methodology for T_{mrt} estimation from weather station and radiation satellite-derived data representative from standar weather station locations) is available in https://zenodo.org/records/13685435.

References

Antonopoulos C, Gilbride T, Margiotta E, Kaltreider C (2022) Guide to Determining Climate Zone by County: IECC and Building America 2021 Updates. https://doi.org/10.2172/1893981

Asaeda T, Ca VT (1993) The subsurface transport of heat and moisture and its effect on the environment: A numerical model. Bound-Layer Meteorol 65(1):159–179. https://doi.org/10.1007/BF00708822

Bai L, Yang L, Song B, Liu N (2020) A new approach to develop a climate classification for building energy efficiency addressing Chinese climate characteristics. Energy 195:116982

Baldwin J, Tarik B, Ebi KL, Ollie J, Lutsko N, Vanos JK (2024) Humidity's role in heat-related health outcomes: a heated debate. Environ Health Perspect 131(5):55001. https://doi.org/10.1289/EHP11807

Baniassadi A, Sailor DJ, Scott Krayenhoff E, Broadbent AM, Georgescu M (2019) Passive survivability of buildings under changing urban climates across eight US cities. Environ Res Lett 14(7). https://doi.org/10.1088/1748-9326/ab28ba

Barriopedro D, Ordóñez C, Miralles DG (2023) Heat waves : physical understanding and scientific challenges. Rev Geophys 61(2). https://doi.org/10.1029/2022RG000780

Bouchama A, Abuyassin B, Lehe C, Laitano O, Jay O, O'Connor FG, Leon LR (2022) Classic and exertional heatstroke. Nat Rev Dis Prim 8(1). https://doi.org/10.1038/s41572-021-00334-6

Bröde P, Fiala D, Błażejczyk K, Holmér I, Jendritzky G, Kampmann B, Tinz B, Havenith G (2012) Deriving the operational procedure for the Universal Thermal Climate Index (UTCI). Int J Biometeorol 56(3):481–494. https://doi.org/10.1007/s00484-011-0454-1

Candas V, Libert J, Vogt J (1979) Human skin wettedness and evaporative efficiency of sweating. J Appl Physiol 43(3):522–528

Cramer MN, Jay O (2019) Cores of reproducibility in physiology partitional calorimetry. J Appl Physiol 126(2):267–277. https://doi.org/10.1152/japplphysiol.00191.2018

Cramer MN, Huang M, Moralez G, Crandall CG (2020) Keeping older individuals cool in hot and moderately humid conditions: wetted clothing with and without an electric fan. J Appl Physiol 128(3):604–611. https://doi.org/10.1152/japplphysiol.00786.2019

Cramer MN, Gagnon D, Laitano O, Crandall CG (2022) Human temperature regulation under heat stress in health, disease, and injury. Physiol Rev 102(4):1907–1989. https://doi.org/10.1152/PHYSREV.00047.2021

Davies-Jones R (2008) An efficient and accurate method for computing the wet-bulb temperature along pseudoadiabats. Mon Weather Rev 136(7):2764–2785. https://doi.org/10.1175/2007MWR2224.1

de Freitas CR (2015) Weather and place-based human behavior: recreational preferences and sensitivity. Int J Biometeorol 59(1):55–63. https://doi.org/10.1007/s00484-014-0824-6

de Freitas CR, Grigorieva EA (2015) A comprehensive catalogue and classification of human thermal climate indices. Int J Biometeorol 59(1):109–120. https://doi.org/10.1007/s00484-014-0819-3

de Freitas CR, Grigorieva EA (2017) A comparison and appraisal of a comprehensive range of human thermal climate indices. Int J Biometeorol 61(3):487–512. https://doi.org/10.1007/s00484-016-1228-6

Dunn RJH (2019) HadISD version 3: monthly updates. https://digital.nmla.metoffice.gov.uk/download/file/digitalFile_13890750-fb6f-42c7-92df-1c4504621fae. Accessed 04/09/2024

Ebi KL, Capon A, Berry P, Broderick C, de Dear R, Havenith G, Honda Y, Kovats RS, Ma W, Malik A, Morris NB, Nybo L, Seneviratne SI, Vanos J, Jay O (2021) Hot weather and heat extremes: health risks. The Lancet 398(10301):698–708. https://doi.org/10.1016/S0140-6736(21)01208-3

Fiala D, Havenith G, Bröde P, Kampmann B, Jendritzky G (2012) UTCI-Fiala multi-node model of human heat transfer and temperature regulation. Int J Biometeorol 56(3):429–441. https://doi.org/10.1007/s00484-011-0424-7

Fonseca-Rodríguez O, Adams RE, Sheridan SC, Schumann B (2023) Projection of extreme heat- and cold-related mortality in Sweden based on the spatial synoptic classification. Environ Res 239(Pt 2):117359. https://doi.org/10.1016/j.envres.2023.117359

Foster J, Smallcombe J, Hodder S, Jay O, Flouris A, Nybo L, Havenith G (2021) An advanced empirical model for quantifying the impact of heat and climate change on human physical work capacity. Int J Biometeorol 65(7):1215–1229. https://doi.org/10.1007/s00484-021-02105-0

Foster J, Smallcombe J, Hodder S, Jay O, Flouris A, Nybo L, Havenith G (2022a) Quantifying the impact of heat on human physical work capacity; part III: the impact of solar radiation varies with air temperature, humidity, and clothing coverage. Int J Biometeorol 66(1):175–188. https://doi.org/10.1007/s00484-021-02205-x

Foster J, Smallcombe J, Hodder S, Jay O, Flouris AD, Havenith G (2022b) Quantifying the impact of heat on human physical work capacity; part II: the observed interaction of air velocity with temperature, humidity, sweat rate, and clothing is not captured by most heat stress indices. Int J Biometeorol 66(3):507–520. https://doi.org/10.1007/s00484-021-02212-y

Greene S, Kalkstein LS, Mills DM, Samenow J (2011) An Examination of climate change on extreme heat events and climate-mortality relationships in large U.S. Cities. Weather Climate Soc 3(4):281–292. https://doi.org/10.1175/WCAS-D-11-00055.1

Grimmond CSB, Cleugh HA, Oke TR (1991) An objective urban heat storage model and its comparison with other schemes. Atmos Environ. Part B, Urban Atmosphere 25(3):311–326. https://doi.org/10.1016/0957-1272(91)90003-W

Grundstein A, Vanos J (2020) There is no 'Swiss Army Knife' of thermal indices: the importance of considering 'why?' and 'for whom?' when modelling heat stress in sport. Br J Sports Med bjsports-102920. https://doi.org/10.1136/bjsports-2020-102920

Gupta R, Mathur J, Garg V (2023) Assessment of climate classification methodologies used in building energy efficiency sector. Energy Build 298:113549

Guzman-Echavarria G, Middel A, Vanos J (2022) Beyond heat exposure — new methods to quantify and link personal heat exposure, stress, and strain in diverse populations and climates: The journal temperature toolbox. Temperature 10(03):358–378. https://doi.org/10.1080/23328940.2022.2149024

Guzman-Echavarria G, Vanos J (2023) PyHHB: Physiological-based estimations of human survivability and liveability to heat in a changing climate (Nature communications (1.0.0)). Zenodo. https://doi.org/10.5281/zenodo.10020137

Havenith G, Fiala D, Błazejczyk K, Richards M, Bröde P, Holmér I, Rintamaki H, Benshabat Y, Jendritzky G (2012) The UTCI-clothing model. Int J Biometeorol 56(3):461–470. https://doi.org/10.1007/s00484-011-0451-4

Holdridge LR (1947) Determination of world plant formations from simple climatic data. Science (New York, N.Y.) 105(2727):367–368. https://doi.org/10.1126/science.105.2727.367

Höppe P (1994) A new procedure to determine the mean radiant temperature outdoors. Wetter Unt Leben 44:147–151

Horton RM, de Sherbinin A, Wrathall D, Oppenheimer M (2021) Assessing human habitability and migration. Science 372(6548):1279–1283. https://doi.org/10.1126/science.abi8603

Ioannou LG, Mantzios K, Tsoutsoubi L, Notley SR, Dinas PC, Brearley M, Epstein Y, Havenith G, Sawka MN, Bröde P, Mekjavic IB, Kenny GP, Bernard TE, Nybo L, Flouris AD (2022) Indicators to assess physiological heat strain–Part 1: Systematic review. Temperature 00(00):1–36. https://doi.org/10.1080/23328940.2022.2037376

Jay O, Capon A, Berry P, Broderick C, de Dear R, Havenith G, Honda Y, Kovats RS, Ma W, Malik A, Morris NB, Nybo L, Seneviratne SI, Vanos J, Ebi KL (2021) Reducing the health effects of hot weather and heat extremes: from personal cooling strategies to green cities. Lancet 398(10301):709–724. https://doi.org/10.1016/S0140-6736(21)01209-5

Khomenok GA, Hadid A, Preiss-Bloom O, Yanovich R, Erlich T, Ron-Tal O, Peled A, Epstein Y, Moran DS (2008) Hand immersion in cold water alleviating physiological strain and increasing tolerance to uncompensable heat stress. Eur J Appl Physiol 104(2):303–309. https://doi.org/10.1007/s00421-008-0693-y

Köppen W (1884) Die Wärmezonen der Erde, nach der Dauer der heissen, gemässigten und kalten Zeit und nach der Wirkung der Wärme auf die organische Welt betrachtet. Meteorol Z 1(21):5–226

Kotthaus S, Smith TEL, Wooster MJ, Grimmond CSB (2014) Derivation of an urban materials spectral library through emittance and reflectance spectroscopy. ISPRS J Photogramm Remote Sens 94:194–212. https://doi.org/10.1016/j.isprsjprs.2014.05.005

Krayenhoff ES, Moustaoui M, Broadbent AM, Gupta V, Georgescu M (2018) Diurnal interaction between urban expansion, climate change and adaptation in US cities. Nat Clim Chang 8(12):1097–1103

Kuras E, Richardson MB, Calkins MM, Ebi KL, Hess JJ, Kintziger KW, Jagger MA, Middel A, Scott AA, Spector JT, Uejio CK, Vanos JK, Zaitchik BF, Gohlke JM, Hondula DM (2017) Opportunities and challenges for personal heat exposure research. Environ Health Perspect 125(8). https://doi.org/10.1289/EHP556

Larose J, Boulay P, Sigal RJ, Wright HE, Kenny GP (2013) Age-related decrements in heat dissipation during physical activity occur as early as the age of 40. PLoS ONE 8(12):e83148. https://doi.org/10.1371/journal.pone.0083148

Larsen L, Gronlund CJ, Ketenci KC, Harlan SL, Hondula DM, Stone B, Lanza K, Mallen E, Wright MK, O'Neill MS (2022) Safe at home?: a comparison of factors influencing indoor residential temperatures during warm weather among three cities. J Am Plan Assoc 0(0):1–13. https://doi.org/10.1080/01944363.2022.2087724

Lee CC (2020) The gridded weather typing classification version 2: A global-scale expansion. Int J Climatol 40(2):1178–1196

Leon LR, Bouchama A (2015) Heat stroke. Compr Physiol 5(2):611–647. https://doi.org/10.1002/cphy.c140017

Lindberg F, Holmer B, Thorsson S (2008) SOLWEIG 1.0 - Modelling spatial variations of 3D radiant fluxes and mean radiant temperature in complex urban settings. Int J Biometeorol 52(7):697–713. https://doi.org/10.1007/s00484-008-0162-7

Liss A, Koch M, Naumova EN (2014) Redefining climate regions in the United States of America using satellite remote sensing and machine learning for public health applications. Geospat Health 8(3):S467–S659

Lstiburek JW (2000) Environmental Loads. Eighth Canadian Building Science Technology Conference

Manu S, Shukla Y, Rawal R, Thomas LE, de Dear R (2016) Field studies of thermal comfort across multiple climate zones for the subcontinent: India Model for Adaptive Comfort (IMAC). Build Environ 98:55–70. https://doi.org/10.1016/j.buildenv.2015.12.019

Mao C, Baltazar JC, Haberl JS (2018) Literature review of building peak cooling load methods in the United States. Sci Technol Built Environ 24(3):228–237. https://doi.org/10.1080/23744731.2017.1373700

MCDPH (2024) 2023 Heat Related Deaths Report. www.maricopa.gov/ArchiveCenter/ViewFile/Item/5820#:~:text=Maricopa County identified a total,related deaths were heat caused. Accessed 04/09/2024

Middel A, AlkhaLed S, Schneider FA, Hagen B, Coseo P (2021) 50 Grades of Shade. Bull Am Meteor Soc 102(9):E1805–E1820. https://doi.org/10.1175/BAMS-D-20-0193.1

Middel A, Huff M, Krayenhoff ES, Udupa A, Schneider FA (2023) PanoMRT: Panoramic infrared thermography to model human thermal exposure and comfort. Sci Total Environ 859:160301. https://doi.org/10.1016/J.SCITOTENV.2022.160301

Morris NB, Chaseling GK, English T, Gruss F, Bin Maideen MF, Capon A, Jay O (2021) Electric fan use for cooling during hot weather: a biophysical modelling study. Lancet Planet Health 5(6):e368–e377. https://doi.org/10.1016/S2542-5196(21)00136-4

Nazarian N, Lee JKW (2021) Personal assessment of urban heat exposure: A systematic review. Environ Res Lett 16(3). https://doi.org/10.1088/1748-9326/abd350

Nazarian N, Krayenhoff ES, Bechtel B, Hondula DM, Paolini R, Vanos J, Cheung T, Chow WTL, de Dear R, Jay O, Lee JKW, Martilli A, Middel A, Norford LK, Sadeghi M, Schiavon S, Santamouris M (2022) Integrated assessment of urban overheating impacts on human life. Earths Future 10(8). https://doi.org/10.1029/2022EF002682

NYC Department of Health (2024) 2023 NYC Heat-Related Mortality Report. https://a816-dohbesp.nyc.gov/IndicatorPublic/data-features/heat-report-archive/2023/. Accessed 04/09/2024

Oke TR, Mills G, Christen A, Voogt JA (2017) Urban climates, 1st edn. Cambridge University Press. https://doi.org/10.1017/9781139016476

Parsons K (2014) Human Thermal Environments, 3rd edn. CRC Press. https://doi.org/10.1201/b16750

Périard JD, Racinais S, Sawka MN (2015) Adaptations and mechanisms of human heat acclimation: Applications for competitive athletes and sports. Scand J Med Sci Sports 25(S1):20–38. https://doi.org/10.1111/sms.12408

Perkins-Kirkpatrick SE, Lewis SC (2020) Increasing trends in regional heatwaves. Nat Commun 11(1):1–8. https://doi.org/10.1038/s41467-020-16970-7

Prata AJ (1996) A new long-wave formula for estimating downward clear-sky radiation at the surface. Q J R Meteorol Soc 122(533):1127–1151. https://doi.org/10.1002/qj.49712253306

Ravanelli NM, Gagnon D, Hodder SG, Havenith G, Jay O (2017) The biophysical and physiological basis for mitigated elevations in heart rate with electric fan use in extreme heat and humidity. Int J Biometeorol 61(2):313–323. https://doi.org/10.1007/s00484-016-1213-0

Rempel AR, Danis J, Rempel AW, Fowler M, Mishra S (2022) Improving the passive survivability of residential buildings during extreme heat events in the Pacific Northwest. Appl Energy 321(May):119323. https://doi.org/10.1016/j.apenergy.2022.119323

Samuelson H, Baniassadi A, Lin A, Izaga González P, Brawley T, Narula T (2020) Housing as a critical determinant of heat vulnerability and health. Sci Total Environ 720. https://doi.org/10.1016/j.scitotenv.2020.137296

Sengupta M, Xie Y, Lopez A, Habte A, Maclaurin G, Shelby J (2018) The National Solar Radiation Data Base (NSRDB). Renew Sustain Energ Rev 89(March 2018):51–60. https://doi.org/10.1016/j.rser.2018.03.003

Sheridan SC (2002) The redevelopment of a weather-type classification scheme for North America. Int J Climatol 22(1):51–68

Simpson CH (2024) Comment on Havenga et al. (2022): Standard heat stress indices may not be appropriate for assessing marathons. S Afr J Sci 120(1/2). https://doi.org/10.17159/sajs.2024/16445

Thornthwaite CW (1948) An approach toward a rational classification of climate. Geogr Rev 38(1):55–94. http://www.jstor.org/stable/210739

Vanos J, Warland J, Gillespie T, Kenny N (2012) Improved predictive ability of climate-human-behaviour interactions with modifications to the COMFA outdoor energy budget model. Int J Biometeorol 56(6):1065–1074. https://doi.org/10.1007/s00484-012-0522-1

Vanos JK, Kalkstein LS, Sanford TJ (2015) Detecting synoptic warming trends across the US Midwest and implications to human health and heat-related mortality. Int J Climatol 35(1):85–96. https://doi.org/10.1002/joc.3964

Vanos JK, Rykaczewski K, Middel A, Vecellio DJ, Brown RD, Gillespie TJ (2021) Improved methods for estimating mean radiant temperature in hot and sunny outdoor settings. Int J Biometeorol 65(6):967–983. https://doi.org/10.1007/s00484-021-02131-y

Vanos J, Guzman-Echavarria G, Baldwin JW, Bongers C, Ebi KL, Jay O (2023) A physiological approach for assessing human survivability and liveability to heat in a changing climate. Nat Commun 14(1):1–14. https://doi.org/10.1038/s41467-023-43121-5

Vecellio DJ, Wolf ST, Cottle RM, Kenney WL (2022) Evaluating the 35°C wet-bulb temperature adaptability threshold for young, healthy subjects (PSU HEAT Project). J Appl Physiol 132(2):340–345. https://doi.org/10.1152/japplphysiol.00738.2021

Vecellio DJ, Kong Q, Kenney WL, Huber M (2023) Greatly enhanced risk to humans as a consequence of empirically determined lower moist heat stress tolerance. Proc Natl Acad Sci 120(42):e2305427120. https://doi.org/10.1073/pnas.2305427120

VDI (1994) VDI 3789, Part 2: environmental meteorology, interactions between atmosphere and surface; calculation of short-and long wave radiation. VDI/DIN-Handbuch Reinhaltung der Luft, Band 1b, Düsseldorf

Walsh A, Cóstola D, Labaki LC (2017a) Comparison of three climatic zoning methodologies for building energy efficiency applications. Energy Build 146:111–121

Walsh A, Cóstola D, Labaki LC (2017b) Review of methods for climatic zoning for building energy efficiency programs. Build Environ 112:337–350

Wolf TS, Cottle RM, Fisher KG, Vecellio DJ, Larry Kenney W (2023) Heat stress vulnerability and critical environmental limits for older adults. Commun Earth Environ 4(1):486. https://doi.org/10.1038/s43247-023-01159-9

Wolf ST, Folkerts MA, Cottle RM, Daanen HAM, Kenney WL (2021) Metabolism- And sex-dependent critical WBGT limits at rest and during exercise in the heat. Am J Physiol Regul Integr Comp Physiol 321(3):R295–R302. https://doi.org/10.1152/ajpregu.00101.2021